Classical magnetotransport of inhomogeneous conductors

Meera M. Parish* and Peter B. Littlewood
Cavendish Laboratory, Madingley Road, Cambridge CB3 0HE, United Kingdom
(Received 24 May 2005; published 14 September 2005)

We present a model of magnetotransport of inhomogeneous conductors based on an array of coupled four-terminal elements. We show that this model generically yields nonsaturating magnetoresistance at large fields. We also discuss how this approach simplifies finite-element analysis of bulk inhomogeneous semiconductors in complex geometries. We argue that this is an explanation of the observed nonsaturating magnetoresistance in silver chalcogenides and potentially in other disordered conductors. Our method may be used to design the magnetoresistive response of a microfabricated array.

DOI: 10.1103/PhysRevB.72.094417 PACS number(s): 75.47.Pq, 72.20.My, 72.80.Ng

I. INTRODUCTION

The problem of determining the effective conductivity of a classical inhomogeneous medium[1] is an old one, but a comprehensive theory of the magnetotransport in such systems is still far from complete. Moreover, much of the early work on inhomogeneous conductors concentrates on the zero-magnetic-field case since this is analogous to calculating the polarization of a random dielectric.[2] For the classical problem to be appropriate, the mean free path of the charge carriers must be much less than the typical length scale of the disorder so that Ohm's law is obeyed locally in space:

$$\mathbf{E}(\mathbf{r}) = \hat{\rho}(\mathbf{r})\mathbf{j}(\mathbf{r}), \tag{1}$$

where $\mathbf{j}$ is the current density, $\mathbf{E}$ is the electric field, and $\hat{\rho}$ is the resistivity tensor. In the case of a simple conductor that possesses a single charge carrier and isotropic inhomogeneities, the resistivity tensor acquires the following form in a magnetic field H:

$$\hat{\rho} = \rho_0 \begin{pmatrix} 1 & \beta & 0 \\ -\beta & 1 & 0 \\ 0 & 0 & 1 \end{pmatrix}. \tag{2}$$

It is clear that this tensor is characterized by just two parameters: the carrier mobility μ (since the dimensionless variable $\beta \equiv \mu H$) and the scalar resistivity ρ_0. While more complex, anisotropic resistivity tensors have also been considered in the inhomogeneous conductor problem,[3–5] this paper shall be solely concerned with Eq. (2).

For inhomogeneous conductors, the effective resistivity ρ_{eff} is defined by $\langle \mathbf{E} \rangle_v = \rho_{\text{eff}} \langle \mathbf{j} \rangle_v$, where $\langle \cdots \rangle_v$ specifies an average over volume. In the absence of disorder, the magnetoresistance $\Delta R/R \equiv [\rho_{\text{eff}}(H) - \rho_{\text{eff}}(0)]/\rho_{\text{eff}}(0)$ is trivially zero, for arbitrary orientation of the magnetic field. However, in general, the magnetoresistance strongly depends on whether it is transverse or longitudinal, i.e., whether the magnetic field is perpendicular or parallel to the current. Furthermore, any nonzero transverse magnetoresistance must be an even function of field due to the rotational symmetry about the current axis. Thus, $\Delta R/R \propto H^2$ in the low field limit, which is usually defined to be $\beta \ll 1$, but the crossover from the low-field to high-field regime is not always obvious in disordered systems, as will be discussed later.

Some recent experiments[6–15] on the doped silver chalcogenides, $Ag_{2+\delta}Se$ and $Ag_{2+\delta}Te$, have added impetus to the investigation of this problem. Both silver chalcogenides exhibit a positive, transverse magnetoresistance that is a linear function of magnetic field throughout the temperature range 4.5–300 K, with no signs of saturation up to fields of 60 T.[6,7] In particular, the linearity continues down deep into the low-field regime $\beta \ll 1$. Such behavior is not what is seen in conventional semiconductors, where the resistance increases quadratically with increasing magnetic field at low fields and, except in very special circumstances, eventually saturates at fields typically of order 1 T,[16,17] corresponding to $\beta \sim 1$. Since the silver chalcogenides are nonmagnetic compounds, the origin of the large magnetoresistance is unclear, although a quantum theory based on the partial population of one Landau magnetic band has been proposed.[18,19] However, the large range in temperature over which the phenomenon occurs suggests that one should examine large magnetoresistances resulting from classical effects, namely the case where the semiconductor is highly inhomogeneous.

The theoretical study of classically disordered conductors may be divided into two separate classes: Media consisting of two or more distinct phases, separated by sharp boundaries, and systems that possess continuously variable fluctuations in the conductivity. In the first class, solutions for a nonzero magnetic field have been derived for an isotropic medium with a low volume fraction $c \ll 1$ of insulating spherical inclusions,[20,21] and they give a positive linear magnetoresistance in the high field limit $\beta \gg 1$, but the increase of the magnetoresistance $\Delta R/R$ with field is small, being proportional to c. An effective medium method has been used to extend this solution to higher volume fractions,[22] but this result is approximate and it is still only applicable to high fields $\beta \gg 1$. The class of systems with continuously varying conductivity fluctuations has only been studied for weak, short-range disorder.[3,23] Using an advection-diffusion analogy, the effective magnetoresistance is determined to be $\Delta R/R \sim \gamma^{4/3}\beta^{2/3}$ for $\beta\gamma \gg 1$, where the disorder width $\gamma \ll 1$.

Thus, the main limitation of the current literature is that it is generally restricted to media that only deviate slightly from homogeneity, so the increase in magnetoresistance is small and anomalous behavior only occurs at very high mag-

netic fields. Whilst there is an exact solution for the effective magnetoresistance in two dimensions that yields a linear magnetoresistance, it is restricted to the special case of a two-component media with equal proportions of each phase.[24–26] However, this does lend credence to the hypothesis that classical disorder is the cause of the anomalous magnetoresistance of the silver chalcogenides.

In order to attack the problem of strong inhomogeneities, we previously introduced a two-dimensional random resistor network model.[27] We used it to show that classical disorder is a possible cause of the anomalous magnetoresistance of the silver chalcogenides, and we raised the possibility of using the networks to construct magnetic field sensors that operate on principles similar to extraordinary magnetoresistance (EMR) devices.[28,29]

In this paper, we investigate the galvanomagnetic properties of the random resistor network model in detail. This model allows one to study the magnetoresistance of an inhomogeneous semiconductor across the whole magnetic field range for a variety of disorder. By considering voltages and current paths within the network, as well as network magnetoresistances, we demonstrate that our resistor network is also capable of simulating macroscopic media with complicated boundaries. We use this result to include contact effects between resistors within the network.

The paper is organized as follows: Section II describes the random resistor network model and derives expressions for the network magnetoresistance and Hall resistance. In Sec. III, we use the insight gained from studying the characteristics of small networks to ascertain the symmetries of the network magnetoresistance and, thus, determine the condition for which the magnetoresistance is nonsaturating. Next, we examine larger networks by studying the magnetotransport of uniform square networks and random square networks in Sec. IV. Finally, we address the ramifications of contact resistances between resistors and boundary effects within the resistor network in Sec. V, before concluding in Sec. VI.

II. RESISTOR NETWORK MODEL

We tackle the inhomogeneous conductor problem by discretizing the medium into a random resistor network and analysing it numerically. Standard resistor networks, where the network unit is taken to be a two-terminal homogeneous resistor, are inadequate for simulating current flow in a magnetic field, since it does not allow the current to flow perpendicular to the voltage drop across a resistor. Thus, a network of two-terminal resistors will not faithfully represent Eq. (2), which requires the local current to make an angle $\arctan(\beta)$ with the local electric field.

The simplest resistor network model that takes account of the Hall component is a two-dimensional square lattice constructed of four-terminal resistors, with a magnetic field applied perpendicular to the network. This is sufficient for simulating a transverse magnetoresistance, but not a longitudinal one since this requires a three-dimensional network. Networks with multi-terminal elements have also been used to study percolating media in a magnetic field[30] but, unlike our model, the elements were restricted to being either insulators or conductors of a set conductivity.

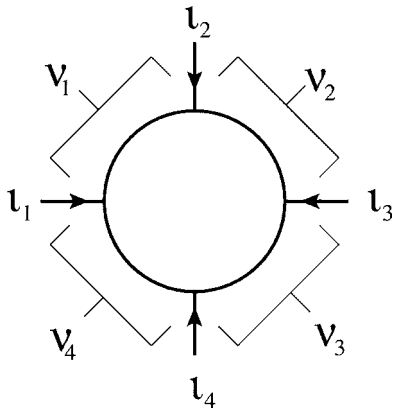

FIG. 1. The network resistor unit consists of a homogeneous, conducting disk with four equally spaced terminals. Currents ι entering the disk are taken to be positive, while the voltage differences ν between the terminals are considered positive when measured in the clockwise direction.

In principle, the network resistor unit can be of arbitrary geometry but, for simplicity, we take it to be a homogeneous circular disk with four current terminals and four voltage differences between the terminals, as shown in Fig. 1. These currents and voltages are related via a 4×4 matrix z:

$$\nu_i = z_{ij}\ \iota_j. \tag{3}$$

The coefficients z_{ij} can be determined by solving the Laplace equation for the electric potential of a homogeneous, conducting disk, using the currents as boundary conditions (see the Appendix). Note that this formulation implicitly assumes a *uniform* injection of current into the terminals at all magnetic fields. In practice, a magnetic field generally perturbs the current at a boundary between two different conductors, but we shall neglect these corrections for now, and revisit them later in our discussion of boundary effects in Sec. V.

If the terminals are taken to be equally spaced and the angular width φ of the terminal is held fixed (we will take $\varphi=0.14$ radians in this paper), then the resistor impedance matrix has the form:

$$z = \frac{\rho}{\pi t}\begin{pmatrix} a & b & c & d \\ d & a & b & c \\ c & d & a & b \\ b & c & d & a \end{pmatrix}. \tag{4}$$

Here, ρ is the disk scalar resistivity and t is the disk thickness, while the matrix elements are dependent on φ and β: $a=-g(\varphi)+(\pi/4)\beta$, $b=g(\varphi)+(\pi/4)\beta$, $c=0.35-(\pi/4)\beta$ and $d=-0.35-(\pi/4)\beta$. In the limit $\varphi\to0$, the function $g(\varphi)\to\infty$ so that the disk resistance diverges as expected. Like Eq. (2), the impedance matrix z of each resistor is characterized by two independent parameters: the mobility μ and the quantity $s=\rho/(\pi t)$. Note that the cyclical permutation of matrix elements is associated with any n-terminal resistor that is invariant under rotations of $2\pi/n$ radians. There is also the added constraint that $\Sigma_i\nu_i=0$, so we have $a+b+c+d=0$.

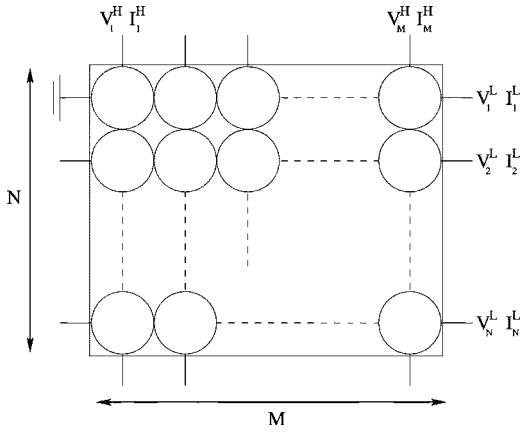

FIG. 2. Schematic diagram of an $N \times M$ network. One terminal is grounded to provide a point of reference for the voltages, and we can disregard the current at the grounded terminal by imposing current conservation. Voltages and currents can be classified into $2N-1$ longitudinal components V_i^L, I_i^L and $2M$ Hall components V_i^H, I_i^H.

To construct an $N \times M$ random resistor network, we connect the disks together (e.g., using perfectly conducting wires) and then vary μ and s for each resistor. Note that we can include positive charge carriers (holes) by allowing μ to be positive as well as negative, whereas previous studies of inhomogeneous media have generally focused on charge carriers of the same sign. In the context of real materials such as the silver chalcogenides, we can view the network as representing an array of silver-ion clusters and voids within the semiconductor.

A typical $N \times M$ network is depicted in Fig. 2. One can define a network impedance matrix Z so that the input voltages $V_i = Z_{ij} I_j$, where I corresponds to the input currents. The impedance matrix is determined by grounding one terminal to provide a point of reference for the voltages, and then using Kirchoff's laws to eliminate the current at the grounded terminal as well as eliminating the internal currents and voltages within the network. By classifying the voltages and currents into $2N-1$ longitudinal components V_i^L, I_i^L, and $2M$ Hall components V_i^H, I_i^H, the $(2M+2N-1) \times (2M+2N-1)$ impedance matrix Z can be written as

$$Z = \begin{pmatrix} Z^{HH} & Z^{HL} \\ Z^{LH} & Z^{LL} \end{pmatrix}. \tag{5}$$

To determine the magnetoresistance of an $N \times M$ network, we set $I_i^H = 0$ and completely ground the left side of the longitudinal voltages in Fig. 2 while setting V^L on the right side to a constant potential U. The network resistance $R_{NM}(H)$ is then given by:

$$R_{NM}(H) = \frac{U}{\sum_i^N I_i^L} = \frac{U}{\sum_i^N (Z^{LL})_{ij}^{-1} V_j^L}, \tag{6}$$

where the sum over input currents is performed along the ungrounded (right) edge. Similarly, the Hall voltages are

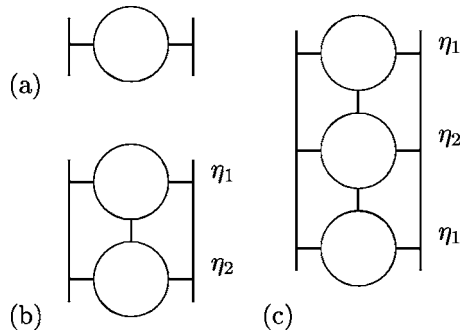

FIG. 3. Examples of small resistor networks corresponding to (a) a single resistor, (b) 2×1 network and (c) 3×1 network, where $\eta_i \equiv (s_i, \mu_i)$.

$$V^H = Z^{HL} (Z^{LL})^{-1} V^L. \tag{7}$$

If we keep the ratio N/M constant and take the limit where $N \to \infty$, then the resistor network should give us the galvanomagnetic properties of a real material. Equation (6) is difficult to solve analytically for large networks and, in practice, we just use Kirchoff's laws to numerically solve for all the currents and voltages in the network, since this allows us to study the current flow and voltage landscape within a network. However, considerable insight can be gained from examining the symmetries of Z.

III. SMALL NETWORKS AND NETWORK SYMMETRIES

In order to elucidate the basic properties of the resistor network model, we begin by studying small networks, namely $1 \times M$ and $N \times 1$ networks. The simplest network is a single resistor, shown in Fig. 3(a), and this yields $\Delta R/R = 0$ as expected, because we have assumed that the disk is a conventional conductor with no implicit magnetoresistance. Moreover, this behavior holds for generic $1 \times M$ networks which are simply equivalent to chains of two-terminal resistors. However, $N \times 1$ networks exhibit nontrivial behavior since they allow for a plurality of current paths within the network when $N > 1$. A 2×1 network of identical resistors [$\eta_1 = \eta_2$ in Fig. 3(b)] yields $\Delta R/R \propto \beta^2$ while a 3×1 network of identical resistors gives a nonzero magnetoresistance that saturates when $\beta \gg 1$. Figure 4 reveals that among uniform $N \times 1$ networks there is a general trend for even-N networks to have a nonsaturating magnetoresistance and for odd-N networks to possess a saturating magnetoresistance, where the saturation level $\Delta R(\infty)/R$ scales as N^2. We see that the differences in $\Delta R/R$ between odd-N and even-N networks diminish as N increases, with N and $N+1$ lying on the same curve for sufficiently small β. However, note that the $N \times 1$ network does not represent a well-defined system in the infinite-N limit since $R_{N1}(0) \to 0$.

Studies of $N \times 1$ networks consisting of two types of resistors have also yielded interesting patterns in the high field behaviour of $\Delta R/R$. For the 2×1 network shown in Fig. 3(b), the magnetoresistance saturates when $s_1 \mu_1 \neq s_2 \mu_2$, where the saturation value of $\Delta R/R$ depends on $(s_1 \mu_1 - s_2 \mu_2)$, but setting $\mu_1 \neq \mu_2$ and $s_1 \mu_1 = s_2 \mu_2$ always gives a

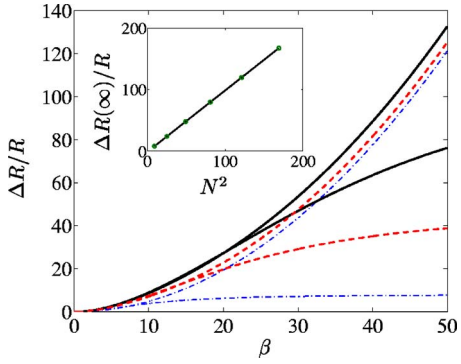

FIG. 4. (Color online) Magnetoresistance of uniform $N\times 1$ networks with set μ,s, where the saturating curves correspond to $N=3$, 7, and 11, in order of increasing size. The remaining curves represent $N=2$, 6, and 10, in order of size again. Inset: For odd N the saturation level $\Delta R(\infty)/R \simeq N^2$.

nonsaturating magnetoresistance. Another example is the 3×1 network in Fig. 3(c) which always has a saturating magnetoresistance except when $s_1\mu_1=2s_2\mu_2$. Similar patterns occur in networks of larger N.

The emergence of these symmetries can be understood by considering the impedance matrix Z. One can demonstrate that it has the form:

$$Z = S + \beta A, \tag{8}$$

where S and A are symmetric and antisymmetric matrices, respectively. For chains of resistors, including the case where we only have one resistor, S and A are always independent of β, but in general they are only constant in the limits where $\beta\to 0$ and $\beta\to\infty$. Note that Z must always be a symmetric matrix at zero magnetic field, since an antisymmetric matrix implies dissipationless current flow. To see this, consider the power of the network

$$P = V^T I = I^T V = I^T Z^T I = I^T Z I.$$

Thus, we have $P=0$ if $Z^T=-Z$. Since the presence of a magnetic field induces dissipationless flow, it makes physical sense to have an antisymmetric matrix attached to β.

The relevant quantity that is used to derive the magnetoresistance is the $(2N-1)\times(2N-1)$ matrix Z^{LL}. From Eq. (5), it also has the form $Z^{LL}=S^{LL}+\beta A^{LL}$. We can write $Z^{LL}=\beta Z_\beta$ so that $Z_\beta\to A^{LL}$ as $\beta\to\infty$. Moreover, A^{LL} is an odd antisymmetric matrix for all N, so Z_β will possess at least one eigenvalue that approaches zero at large fields.

Now, the sum of the input currents along the right edge can be written as

$$\sum_i^N I_i^L = \frac{1}{\beta}\sum_i^N \sum_n^{2N-1} \frac{w_{n,i}w_{n,j}^T}{\lambda_n} V_j^L, \tag{9}$$

where w_n and λ_n are the nth eigenvector and eigenvalue of Z_β, respectively. Since β appears in the denominator, all terms will vanish in the high field limit except for the singular terms associated with the eigenvalues approaching zero. Their behavior will determine whether the magnetoresistance is saturating or nonsaturating. If we assume that only one eigenvalue λ_0 approaches zero in the high field limit, then we have

$$\sum_i^N I_i^L \simeq \frac{U}{\beta\lambda_0}\left(\sum_i^N w_{0,i}\right)^2 + O\left(\frac{1}{\beta}\right). \tag{10}$$

The behavior of λ_0 is governed by S^{LL}/β so we must have $\lambda_0\propto 1/\beta$ when $\beta\gg 1$. Therefore, λ_0 cancels β in the denominator and the magnetoresistance is only nonsaturating if $\Sigma_i^N w_{0,i}\to 0$ at large fields. This explains why special configurations of resistors in the small networks give a nonsaturating magnetoresistance. In the case where the magnetoresistance is saturating, λ_0 dominates the electrical transport and $I_i^L \to w_{0,i}$. More generally, $\Sigma_i^N w_{0,i}$ will determine the exact dependence of $R_{NN}(H)$ on field as $\beta\to\infty$.

To be more concrete, let us consider the simple case where

$$A^{LL} = \begin{pmatrix} \mathbf{0} & \mathbf{1} \\ \mathbf{-1} & \mathbf{0} \end{pmatrix}. \tag{11}$$

Then the zero eigenvalue has the (normalized) eigenvector $w_{0i}=(-1)^i/\sqrt{2N-1}$ and in the high field limit we obtain

$$\sum_i^N I_i^L \propto \frac{U}{2N-1}\left[\left(\sum_i^N (-1)^i\right)^2 + \delta(\beta,N)\right], \tag{12}$$

where $\delta(\beta,N)$ is a finite-field correction factor that vanishes as $\beta\to\infty$. Therefore, we have the high-field resistance

$$R_{NN}(H) \propto \begin{cases} 2N-1 & \text{if } N \text{ is odd} \\ \dfrac{2N-1}{\delta(\beta,N)} & \text{if } N \text{ is even.} \end{cases} \tag{13}$$

The magnetoresistance is nonsaturating for even-N networks and it saturates for odd-N networks, in agreement with Fig. 4. The fact that $R_{NN}(H)$ scales linearly with N for odd-N networks is in apparent contradiction with the inset of Fig. 4, but consistency is recovered once one notes that $R(0)\propto 1/N$ so that, at high fields, $R_{NN}(H)/R(0)\propto N^2$ for $N>1$.

Since Eq. (13) is independent of M, we expect it to be valid for all uniform networks. However, in the case of large random networks, the situation is more complicated since there is generally a distribution of eigenvalues that approaches zero at high fields. This must be properly treated using sophisticated tools such as random matrix theory.

IV. LARGE SQUARE NETWORKS

To investigate larger networks, we focus on $N\times N$ networks because their zero-field resistance remains finite as $N\to\infty$. Of course, a finite zero-field resistance is obtained for any $N\times M$ network provided we keep the ratio N/M constant as $N\to\infty$, but square networks are chosen for numerical convenience.

A. Uniform resistor networks

The simplest square network is where all the resistors are identical and in this case the zero-field resistance is constant

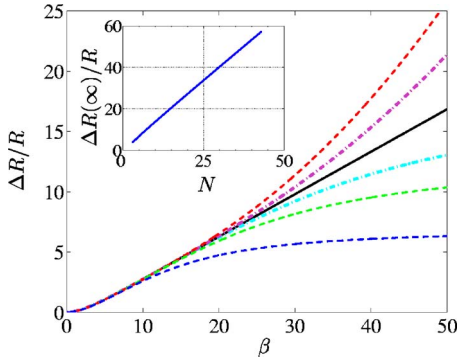

FIG. 5. (Color online) Magnetoresistance of $N\times N$ uniform networks, where the saturating dotted curves correspond to $N=5$, 9, and 13, in order of increasing size, and the remaining dotted curves are $N=10$ and 14 as curve size decreases. The solid curve represents the straight line $\Delta R/R \simeq 0.35\beta$ that the dotted curves collapse onto when $1<\beta<2N$. Inset: For odd N the saturation level $\Delta R(\infty)/R \simeq 1.4N$.

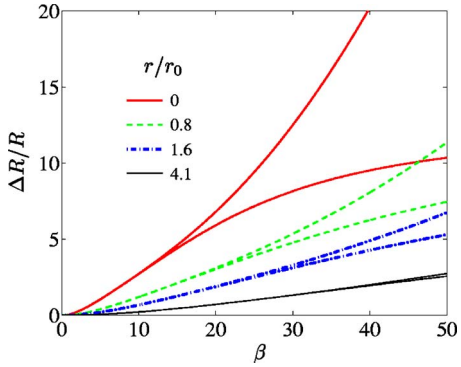

FIG. 6. (Color online) Magnetoresistance of 9×9 and 8×8 uniform networks, where there is a constant resistance r at the connections between elements. Note that $\Delta R/R$ of the 8×8 network corresponds to the larger curve at given r. The unit in which r is measured, r_0, is taken to be $R(0)$ of a uniform square network with $r=0$.

as system size is increased. In accordance with Eq. (13), uniform square networks retain the "odd-even" trend of $N\times 1$ networks, where odd-N networks display a saturating magnetoresistance and even-N networks exhibit a nonsaturating one (see Fig. 5). The key difference is that the $\Delta R/R$ curves collapse onto a straight line for $\beta>1$ as $N\to\infty$, while there are no changes to the low field ($\beta<1$) behavior, where $\Delta R/R \propto \beta^2$. This nonsaturating, linear behavior resembles the magnetoresistance of the silver chalcogenides and it makes large networks candidates for sensors of high magnetic fields. Note that $\Delta R/R$ is independent of s since it just appears as a scaling of $R(H)$ in uniform networks. From the inset of Fig. 5, we see that the magnetoresistance saturation of odd networks scales linearly with N as expected.

From the point of view of experimentally constructing $N\times N$ uniform networks, it is worth examining the effect of adding a finite resistance r at the connections between elements. One can mathematically show that this is, in fact, equivalent to reducing the angular width φ of the terminals. From our numerical simulations, we find that it does not change whether the magnetoresistance is saturating or otherwise, but in Fig. 6 we see that the size of $\Delta R/R$ at a given field decreases with increasing r. Additionally, it changes the field scale such that the divergence of odd and even curves, as well as the crossover from linear to quadratic behaviour, is shifted to higher fields. The reduction in $\Delta R/R$ as r increases is not surprising, because in the limit where $r\to\infty$, the Ohmic dissipation in the network is dominated by the connections between disks and we effectively recover a network of two-terminal resistors, which has $\Delta R/R=0$.

Another important characterization of uniform networks is the Hall coefficient R^H. In terms of network parameters (see Fig. 2), we have

$$R_j^H = \frac{V_j^H - V_{M+j}^H}{H\sum_i I_i^L}, \tag{14}$$

where it is a function of the position across the network $j=1,2,\ldots,M$. By symmetry, we expect $R_j^H = R_{M+1-j}^H$. The Hall coefficient converges rapidly with increasing system size, so we will restrict our consideration to uniform 16×16 networks. In Fig. 7, we observe that it has the general form $R_j^H = s\mu f_j(\beta)$ so, if we take $\rho=(ne\mu)^{-1}$, R^H is inversely proportional to carrier density n like conventional semiconductors. In contrast to a conventional semiconductor, it is also dependent on β at low fields and the strength of this dependency increases as we approach the network edges $j=1$, 16. This already hints that network boundaries play an important role in the magnetotransport of uniform networks, as will be discussed in Sec. V.

B. Random resistor networks

To model real inhomogeneous conductors, it is necessary to consider random resistor networks. In this case, we take the distribution of μ within the network to be Gaussian, with width $\Delta\mu$. Since s is always positive, we take $s=\eta^2$, where η also has a Gaussian distribution of width $\Delta\eta$. We can then define the width of s to be $\Delta s = \sqrt{\langle\eta^4\rangle - \langle\eta^2\rangle}$, where $\langle\cdots\rangle$ is an average over the Gaussian distribution. A numerical analysis of random $N\times N$ networks produces positive magnetoresistances that depend on the particular network configuration

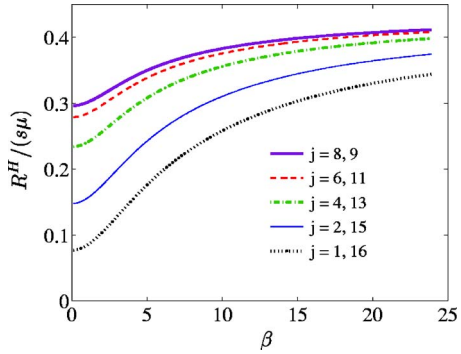

FIG. 7. (Color online) Hall coefficient R_j^H for different positions j across a uniform 16×16 network. It is dependent on μ as well as s, and it has the general form $R_j^H = s\mu f_j(\beta)$.

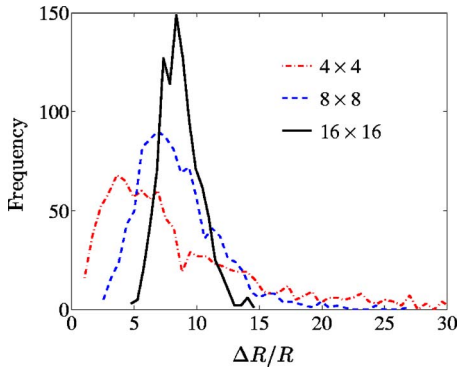

FIG. 8. (Color online) Distributions of magnetoresistance taken from 1000 samples for each network size, where we have set $\langle\mu\rangle=0$, $\Delta\mu H=50$, and $\langle\eta\rangle=0$ (so that $\Delta s/\langle s\rangle=1/\sqrt{2}$).

for small N and, consequently, exhibit a large range in behavior whose variation increases with increasing H. However, this range in behavior diminishes with increasing N, as illustrated in Fig. 8. The distributions of magnetoresistance at large field clearly show a decreasing distribution width as N increases and the distribution becomes evenly spread about the mean for sufficiently large N. Therefore, the magnetoresistance of the infinite random network should be given by the average magnetoresistance of finite networks.

Figure 9 displays our key results for simulations performed on 20×20 random networks. We find that the average $\Delta R/R$ is linearly dependent on field and that it is strongly dependent on μ, but it is still insensitive to s like in the uniform case. This linear dependence can be argued on the grounds that current in a strongly disordered medium at large fields is forced to flow perpendicular to the applied voltage a significant proportion of the time and, therefore, contributes the Hall resistance $\rho_{xy}\propto H$ to the effective magnetoresistance. The character of the mobility distribution determines the size of the relative magnetoresistance because, at sufficiently large magnetic fields, we see that $\Delta R/R\propto\langle\mu\rangle$ for $\Delta\mu/\langle\mu\rangle<1$ and $\Delta R/R\propto\Delta\mu$ for $\Delta\mu/\langle\mu\rangle>1$, where the exact proportionality constants depend on the details of the distribution. Therefore, we would expect $\Delta R/R$ of an inhomogeneous semiconductor to diminish with increasing temperature, since this corresponds to a decrease in μ due to phonon excitations. This is consistent with experiments on the silver chalcogenides.[6]

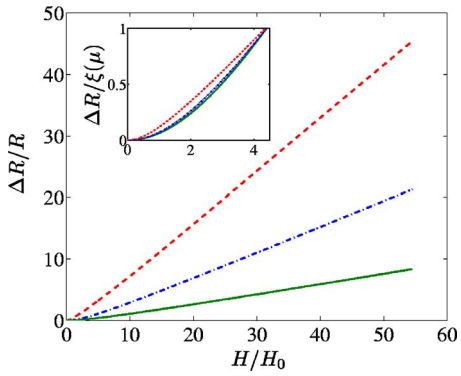

FIG. 9. (Color online) Average magnetoresistance $\Delta R/R$, as a function of dimensionless magnetic field H/H_0, of 20×20 random resistor networks for 3 different mobility distributions, where $H_0=1$ kOe is a typical field scale. The magnetoresistance was averaged over 10 random network configurations and, in order of increasing size, the curves correspond to: (i) $\langle\mu\rangle=0.1H_0^{-1}$, $\Delta\mu=H_0^{-1}$, (ii) $\langle\mu\rangle=H_0^{-1}$, $\Delta\mu=0$, and (iii) $\langle\mu\rangle=0$, $\Delta\mu=5H_0^{-1}$. Inset: By scaling the curves so that they all have the same magnetoresistance at around $4H_0$, it can be seen that linearity continues down to lower fields when the mobility disorder is large, $\Delta\mu\gg H_0^{-1}$.

The crossover from linear to quadratic behavior occurs at field $\langle\mu\rangle^{-1}$ for $\Delta\mu/\langle\mu\rangle<1$ and $(\Delta\mu)^{-1}$ for $\Delta\mu/\langle\mu\rangle>1$. Thus, even when the characteristic field $\langle\mu\rangle^{-1}$ is of order 1 T, the measured crossover field of a disordered semiconductor can be several orders of magnitude smaller, provided $\Delta\mu$ is large. This yields a possible explanation for why the linearity of the silver chalcogenide magnetoresistance continues down to fields as low as 10 Oe.

It is also of interest to determine how disorder affects the Hall coefficient, because experiments on the silver chalcogenides have established that an anomalous universal relationship exists between the magnetoresistance and the Hall resistance.[7] Unfortunately, an enormous range in behavior is displayed for the Hall resistance of finite random networks, and there is no obvious convergence in the behaviour for network sizes $N<30$. Thus, we need to examine even larger networks in order to determine the Hall resistance for the infinite network. One possible approach is to implement a numerical renormalization group technique where each resistor unit is replaced by a new, renormalised resistor unit consisting of a 2×2 resistor network, but this is beyond the scope of this paper.

V. BOUNDARY EFFECTS

A. Effects of macroscopic boundaries

Before we conclude our study of large resistor networks, we need to address an apparent conundrum: The uniform network in the infinite limit should behave like a classical homogeneous conductor with no magnetoresistance. To see this, consider a single resistor, like Fig. 1, within the infinite uniform network. From translational symmetry, current entering the resistor from the right (bottom) terminal is equal to the current leaving from the left (top). If we assume that the current flowing perpendicular to the applied voltage is zero, as dictated by the boundary conditions, then the magnetoresistance of the uniform network becomes equivalent to that of a single resistor, and is thus zero. So why is the magnetoresistance that we calculated for the infinite uniform network nonzero and nonsaturating? The answer lies in boundary effects due to the perfectly conducting electrodes that are used to apply the potential difference across the network.

Figure 10 depicts the boundary between the ideal electrode and a material of finite resistivity ρ_1 in the $x-y$ plane. If a magnetic field H is applied in the z direction, the classical electrical transport in homogeneous material obeys Ohm's law, with a resistivity tensor $\hat{\rho}$ given by Eq. (2). Now, the electric field E_y that is parallel to the surface must be continuous across the boundary according to the standard

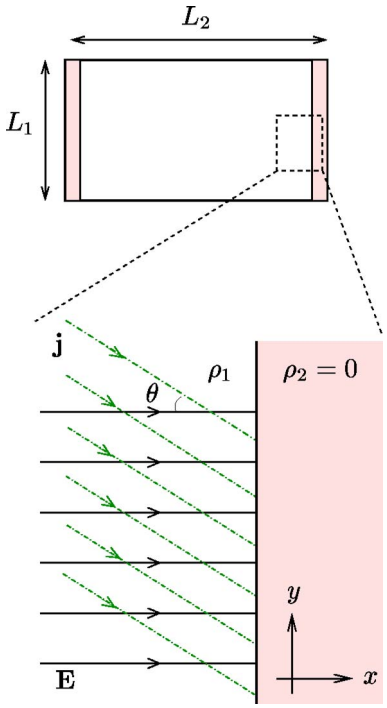

FIG. 10. (Color online) An $L_1 \times L_2$ homogeneous medium with two perfectly conducting electrodes attached. The electrode boundary may be treated as an interface between an ideal conductor and a material with finite resistivity ρ_1. In a magnetic field, current $\boldsymbol{j}$ enters the ideal conductor at an angle $\theta = \arctan \beta$ with respect to the electric field $\mathbf{E}$.

Maxwell equations. Since the electric field inside an ideal conductor is always zero, then $E_y = 0$ and the electric field outside the conductor must, therefore, be perpendicular to the perfectly conducting surface. This, combined with the form of $\hat{\rho}$, causes the current to enter and exit the perfectly conducting electrodes at the angle $\theta = \arctan \beta$. For strong fields $\beta \gg 1$, the current is angled at almost 90° to the electric field, so the effective resistivity of the material close to the electrodes is

$$\rho_{\text{eff}} \simeq \left| \frac{E_x}{j_y} \right| \simeq \rho_1 \beta. \tag{15}$$

This provides an explanation for the linear magnetoresistance of the infinite uniform network in Fig. 5. In general, currents will be perturbed at a boundary that is perpendicular to the $x-y$ plane if there is a mismatch of Hall electric fields E_y across the interface when $j_y = 0$.

Figure 11(a) demonstrates that, in a large uniform network, the current is most strongly perturbed at the electrode boundaries in a strong magnetic field. Deep within the network, away from the boundaries, the current is uniformly spread, so a measurement of the bulk magnetoresistance using a four-probe[31] measurement, will yield a zero magnetoresistance in the infinite size limit. There is also the extra restriction that no current is allowed to enter or leave the top and bottom edges of the network, so this forces the majority of the current to enter the network at the top left corner and leave at the bottom right corner. As $\beta \to \infty$, we obtain singularities of the current in the aforementioned corners. This type of behaviour has already been noted in the context of real homogeneous materials.[32]

In addition, the anomalous Hall coefficient in Fig. 7 qualitatively matches calculations for the response of simple Hall devices constructed from homogeneous materials with a square geometry[33,34] like that in Fig. 10. There, a geometrical correction factor is used to describe the diminution of the Hall voltage due to finite size effects, and this factor is dependent on the ratio of the electrode width L_1 with respect to the length L_2 of the Hall device, i.e., the ratio N/M of an infinite uniform resistor network.

It is important to stress that *random* resistor networks correspond to an entirely different class of system from the homogeneous conductor: The infinite random resistor network represents an inhomogeneous material, while a uniform net-

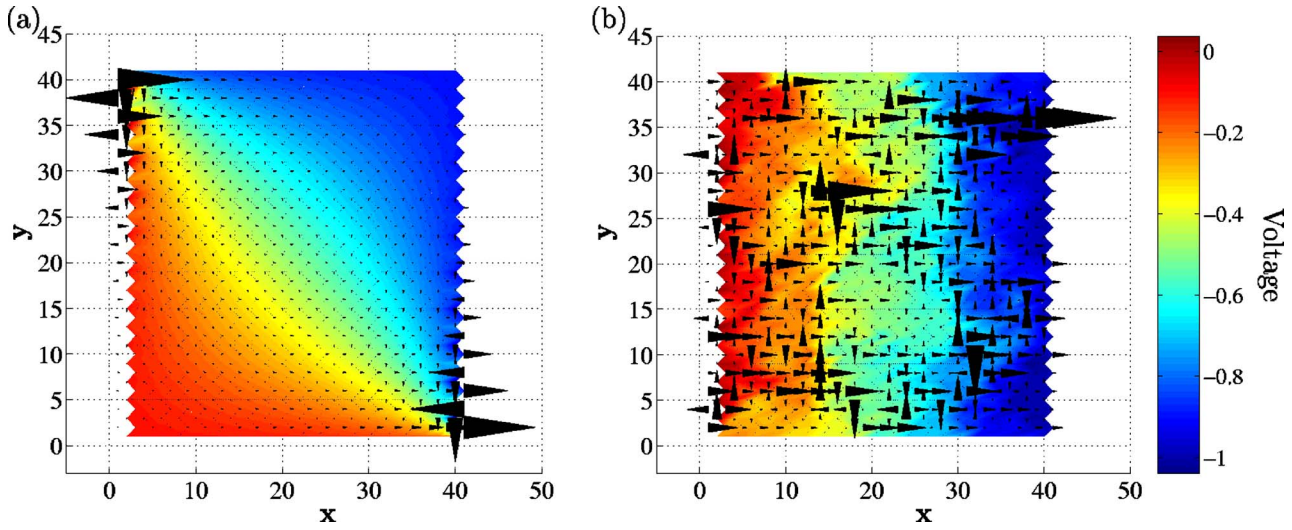

FIG. 11. (Color online) Visualizations of currents and voltages at large field in a 20×20 network of disks with radii 1 (arbitrary units), where the potential difference $U = -1$ V. The black arrows represent currents, where arrow size corresponds to the magnitude of the current. (a) Uniform network at $\beta = 30$. (b) Random network with $\langle \mu \rangle = 0$, $\Delta \mu H = 30$ and $\Delta s / \langle s \rangle = 1/\sqrt{2}$.

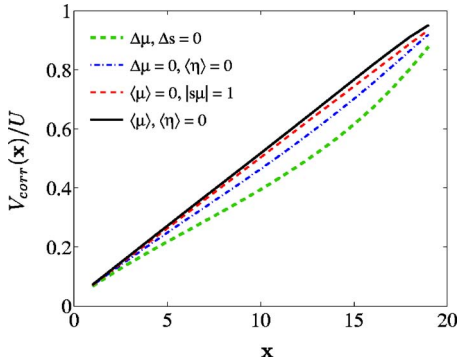

FIG. 12. (Color online) Voltage correlation function at large magnetic field for 20×20 networks of varying disorder. Note that the cases with $\langle\eta\rangle=0$ correspond to $\Delta s=\langle s\rangle/\sqrt{2}$, since $s=\eta^2$. For random networks, the function has been averaged over 100 samples.

work may only be regarded as inhomogeneous when the system size is finite. Comparing Figs. 11(a) and 11(b), we see that the current paths are highly inhomogeneous and filamentary within the random network unlike the uniform case. The voltage landscape is also nontrivial and the current paths create loops within the random system. Therefore, the magnetoresistance should be nonzero deep within the random network, away from the boundaries.

We can strengthen this claim by considering the voltage correlation function:

$$V_{corr}(\mathbf{x}) = \langle V(\mathbf{r}+\mathbf{x}) - V(\mathbf{r})\rangle_{\mathbf{r}}, \tag{16}$$

where $V(\mathbf{r})$ is the voltage at position $\mathbf{r}$ in the network, $\mathbf{x}$ denotes vectors oriented in the x-direction, and $\langle\cdots\rangle_{\mathbf{r}}$ represents an average over $\mathbf{r}$. Taking the radii of the disks to be 1 (arbitrary units), we should note that $V_{corr}(N\hat{x})=U$ in an $N\times N$ network, since this corresponds to measuring the potential difference across the whole network.

Figure 12 plots the voltage correlation function at large magnetic field of 20×20 networks for four different cases of disorder. When the network is uniform, we see that the slope of $V_{corr}(\mathbf{x})$ suddenly increases for large $\mathbf{x}$, which implies that the voltage drops within the network are smaller than those close to the boundary. This demonstrates that much of the magnetoresistance of the network is confined to the boundaries, as expected. In contrast, as we increase the disorder in the network, the behavior of $V_{corr}(\mathbf{x})$ tends to a straight line, indicating that the linear magnetoresistance is spread across the whole of the network and is not just a boundary effect. Of particular interest is the fact that maximum insensitivity to the boundary is achieved when $\langle\mu\rangle=0$, which could imply that the magnetoresistance is largest when electrons and holes are present in equal proportions, as has been measured in experiment.[8] Recent calculations by Guttal and Stroud[26] on two-dimensional, two-phase media further support these observations. They prove that the magnetoresistance of their inhomogeneous conductor is linear when $\langle\mu\rangle=0$, but it can saturate when $\langle\mu\rangle\neq0$, like in experiment.

B. Finite-element modeling of macroscopic media

In addition to studies of random media, there is also interest in understanding classical macroscopic media with complex geometries, because of possible geometrical effects in magnetoresistance and Hall measurements. Geometric enhancements of the magnetoresistance are already the basis of sensitive EMR magnetic-field sensors.[28,29] In general, it is difficult to analytically calculate the magnetotransport of macroscopic media with complicated boundaries, because the calculation involves solving differential equations for the currents/voltages where the boundary conditions contain derivatives that are oblique to the boundary surfaces.[35] Thus, standard mathematical techniques, such as separation of variables, will typically fail in these problems, although the application of conformal mappings in two dimensions has proved successful in dealing with simple geometries.[34,36,37] However, one can, in principle, use infinite uniform networks to simulate two-dimensional, macroscopic, composite conductors, in a manner analogous to the finite-element modeling of EMR devices.[38] Moreover, current perturbations at the connections between disks can be disregarded entirely in these networks if we choose the terminals to have the same resistivity as the disks. Boundaries within the macroscopic system still present a potential problem since they involve disks of differing resistivity connected together. But, at fixed magnetic field, the magnitude of these contact effects will tend to zero as the granularity of the network goes to zero $(N,M\to\infty)$, provided the number of elements with contact effects scales slower than the total number of elements. This is certainly true for one-dimensional boundaries within a two-dimensional homogeneous medium, since the number of boundary elements in the network scales like N while the total number of elements scales like N^2.

It is important to note that the homogeneous conductor constructed from the infinite uniform network will possess a mobility μ^* and resistivity ρ^* that is different from those of the elements that generate the network. Generally, these effective network parameters will depend on the geometry of the element as well as the connections between elements. For the situation where there is no resistance between the elements, the effective quantities can be determined from the resistivity and Hall coefficient of a single element. Therefore, using Eq. (4), we have parameters

$$\rho^* = \frac{2\rho}{\pi t}[g(\varphi)+0.35], \tag{17}$$

$$\mu^* = \frac{\pi\mu}{2[g(\varphi)+0.35]}. \tag{18}$$

The high-field magnetoresistance of the uniform square network in Fig. 5 is then given by $\Delta R/R\sim\mu^* H$.

To confirm the validity of our numerical approach, we can compare the magnetoresistance of infinite uniform networks with results of the conformal mapping approach. Following the method of Rendell and Girvin,[35] we find that the $L_1\times L_2$ homogeneous medium in Fig. 10 has resistance:

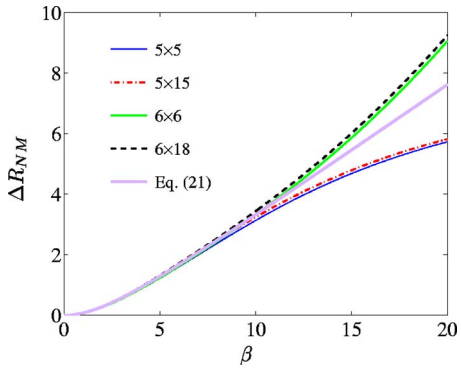

FIG. 13. (Color online) Comparison of resistances from a representative sample of $N \times M$ networks with $M \geqslant N$, where we have defined $\Delta R_{NM} \equiv R_{NM}(H) - R_{NM}(0)$ and we have set $s=1$. These curves approach Eq. (21) in the limit of infinite network size. Curves with $M > 3N$ are indistinguishable from the $M=3N$ curves and are, therefore, not shown.

$$R = \rho_1 \sqrt{1+\beta^2} \frac{\int_0^1 dx \cos \Theta_{L_1 L_2}(x)}{\int_0^1 dx \cos \Theta_{L_2 L_1}(x)}, \tag{19}$$

where

$$\Theta_{L_1 L_2}(x) = \sum_{n(\text{odd})} \frac{4 \arctan(\beta)}{n\pi} \frac{\sin(n\pi x)}{\cosh\left(\frac{n\pi L_1}{2L_2}\right)}.$$

Thus, for the special case where $L_1 = L_2$, we have the exact result $R = \rho_1 \sqrt{1+\beta^2}$, which is in agreement with our numerical simulations of $N \times N$ networks in Fig. 5 if we take $N \to \infty$, $\beta = \mu^* H$ and $\rho_1 = \rho^*$.

For a general $N \times M$ uniform network with $M \geqslant N$, the numerical simulations in Fig. 13 demonstrate that the resistance is approximately given by the expression:

$$R_{NM}(H) \simeq R_{NN}(H) + R_{NN}(0)\left(\frac{M}{N} - 1\right). \tag{20}$$

Thus, in the limit where $N, M \to \infty$, we have resistance

$$R_{NM} \simeq \rho^* \left(\sqrt{1 + (\mu^* H)^2} - 1 + \frac{M}{N} \right). \tag{21}$$

This becomes independent of network dimensions as $H \to \infty$, like previous studies of two-terminal devices have predicted,[39] but the high-field magnetoresistance is $\Delta R/R \propto N/M$ since $R_{NM}(0) = \rho^* M/N$.

C. Contact resistance between elements

The insights gained in the previous section can be used to analyze contact effects between elements in the network. We previously assumed a uniform current injection into the disk terminals, but this is generally difficult to achieve when $\beta \gg 1$. The assumption of uniform current is only valid for all fields when the Hall resistance $\rho\mu$ and thickness t is identical for each element. To assess the ramifications of current perturbations at the disk terminals, we consider the simple case of ideal metal bridges connecting the disks. Our numerical simulations show that current distortions are restricted to the vicinity of the perfectly conducting electrode, while other calculations[40] demonstrate that the lengthscale of the current distortion is proportional to φ. Therefore, when $\varphi \ll 1$, it is legitimate to replace the bridge with a two-terminal resistor possessing a field-dependent resistance. Using our results for a homogeneous conductor with boundaries, we determine the contact resistance between disks i and j to be

$$\rho_c^{ij} = \frac{1}{2}\left(\frac{\rho_i}{t_i} h(\mu_i H) + \frac{\rho_j}{t_j} h(\mu_j H) \right), \tag{22}$$

where we take $h(\beta) = \sqrt{1+\beta^2} - 1$ to obtain the correct low-field and high-field limits.

The contact resistance cannot be eliminated from our network model by reducing the terminal width φ, because the disk impedance coefficients associated with field in Eq. (4) are independent of φ like ρ_c, even though the disk resistance tends to infinity as $\varphi \to 0$. Moreover, in the case of the infinite uniform network at large fields, the contact resistance ρ_c is equal to the network resistance ΔR_{NM} without metallic bridges for *all* $\varphi \ll 1$.

From simulations of random square networks that include this contact resistance, we find that the size of the network magnetoresistance is increased by up to 100% or more, depending on the network disorder, but the major results are qualitatively unchanged: the variation in magnetoresistance decreases with increasing network size like in Fig. 8, the average magnetoresistance is linearly dependent on field, and the crossover point is determined by the mobility distribution, as in Fig. 9. One important consequence of these contact resistances is that the bulk magnetoresistance is always nonsaturating and linear, plus the network's sensitivity to the network boundaries is reduced. For example, an infinite uniform square network with metal bridges will possess a nonzero bulk magnetoresistance of $\rho_c/R(0)$ due to the contacts, and we find that this accounts for about 70% of a two-terminal measurement of the network's magnetoresistance.

Note that contacts of perfectly conducting wires represent an extreme limit where the contact effects are greatest. A potentially richer case is where the wires are replaced by interfaces between elements. Here, the magnitude of each contact resistance in a random network ranges from Eq. (22) right down to zero, when neighboring elements have the same Hall resistance and thickness. Thus, we can expect to recover bulk magnetoresistances, similar to those displayed in Fig. 12, that sensitively depend on network disorder.

The situation is further complicated when we consider three-dimensional effects at the connections between resistors. An interesting example is where the disk resistivity ρ and mobility μ are constant within the network, but s is varied by altering the disk thickness t. Calculations by Bruls *et al.*[41,42] that involve mapping sample thickness variations onto a two-dimensional problem, have shown that sharp changes in thicknesses, like those at the interfaces between resistors, will have resistance

$$\rho_c^{ij} \sim \rho\beta\Delta_{ij}, \tag{23}$$

where $\Delta_{ij} \equiv (t_i - t_j)/t_i$, $t_i \geqslant t_j$ and $\beta\Delta_{ij} \gg 1$. Thus, the contact resistance still has a linear field dependence at large fields, but the size of the effect is reduced so that the assumption of uniform current injection is now valid for $\beta \ll \Delta_{ij}^{-1}$. A thorough analysis of these more complex contact effects will be the subject of future work.

VI. CONCLUSION

In this paper we have modeled an inhomogeneous conductor using a two-dimensional random resistor network that consists of *four*-terminal resistors in order to take account of the Hall component. We have shown that the network impedance matrix Z becomes an odd, antisymmetric matrix at large magnetic field, so that the high-field behavior of the magnetoresistance is determined by the zero eigenvalue of Z. We find that a nonsaturating magnetoresistance can be obtained in networks as small as 2×1, where a plurality of current paths is allowed within the network, while large networks typically possess a linear magnetoresistance. This is in contrast to EMR devices that exhibit an extremely large but saturating magnetoresistance.[28,29]

By considering large square networks, we have demonstrated that uniform networks in the limit of infinite size are equivalent to homogeneous conductors and the observed linear magnetoresistance in this system results from boundary effects at the macroscopic electrodes. As such, they can be used to model macroscopic media with complex boundaries. However, large random networks model strongly inhomogeneous semiconductors and their magnetoresistance is not simply a boundary effect. They correctly reproduce the anomalous magnetoresistance of the silver chalcogenides: Nonsaturating behavior with a linearity that continues down to low fields for large mobility disorder. Moreover, the magnetoresistance may be large when the Hall resistance is zero, like in experiment.

The advantage of such a phenomenological model of positive, nonsaturating magnetoresistance is that it is potentially relevant to a whole range of materials. Already, similar magnetoresistances have been observed in metallic VO_x thin films,[43] micro-sized $Co_x - C_{1-x}$ composites[44] and $LaSb_2$ crystals.[45] Two-dimensional electron gases also show a mysterious linear magnetoresistance[46] and classical disorder has been cited as a possible cause.[47]

A major limitation of our random resistor network model is that it is restricted to two dimensions and, thus, cannot describe longitudinal magnetoresistance. It is also known that weakly disordered systems with continuous fluctuations in the conductivity possess magnetoresistances that depend on the dimensionality.[1] Therefore, we must extend our resistor network model to three dimensions in order to fully simulate an inhomogeneous semiconductor. However, we anticipate that our two-dimensional resistor networks will motivate experiments on the magnetotransport of systems with controlled disorder and on high-field magnetic sensors.

Finally, it would be interesting to explore the magnetothermopower of our resistor networks. A giant magnetothermopower is associated with $Ag_{2-\delta}Te$ samples[48] and its origin may also lie in classical disorder, because experiments on composite semiconductor-metal structures demonstrate that the magnetothermopower can be geometrically enhanced.[49]

ACKNOWLEDGMENTS

We are grateful to Anke Husmann, Tom Rosenbaum, and Nigel Cooper for simulating discussions. M.M.P. acknowledges support from the Commonwealth Scholarship Commission and the Cambridge Commonwealth Trust.

APPENDIX: IMPEDANCE MATRIX OF A 4-TERMINAL CIRCULAR DISK

We begin by writing the electric field in terms of the potential, $\mathbf{E} = -\nabla U$, and then combining charge conservation $\nabla \cdot \mathbf{j} = 0$ with Ohm's law to obtain the following differential equation for the potential:

$$\frac{\partial}{\partial x_i}\left(\sigma_{ik}\frac{\partial U}{\partial x_k}\right) = 0, \tag{A1}$$

where the conductivity tensor $\hat{\sigma} = \hat{\rho}^{-1}$. For the case of a homogeneous medium, Eq. (A1) is simply the Laplace equation.

Consider the homogeneous disk in Fig. 1. If we assume uniform current injection into the terminals, then we can use the currents as the boundary conditions to solve the Laplace equation for the potential. In the absence of a magnetic field, it is sufficient to take $\varphi \ll 1$ in order for this assumption to be valid, but the currents will generally be distorted when $\beta \gg 1$. To simplify the problem, we shall initially neglect these distortions.

Taking the currents entering each terminal to be I_1, I_2, I_3, and I_4, respectively, we then obtain the following potential along the edge of the disk:

$$U(\beta,\theta) = -\frac{\rho}{\pi\varphi t}\sum_{n=1}^{\infty}\frac{1}{n^2}[(S-\beta T)\cos(n\theta) + (T+\beta S)\sin(n\theta)], \tag{A2}$$

where θ defines the angular position on the disk edge, and we have

$$\begin{aligned} S = {} & 2I_1\sin(n\varphi/2) + I_2[\sin(n\pi/2 + n\varphi/2) - \sin(n\pi/2 - n\varphi/2)] \\ & + I_3[\sin(n\pi + n\varphi/2) - \sin(n\pi - n\varphi/2)] \\ & + I_4[\sin(3n\pi/2 + n\varphi/2) - \sin(3n\pi/2 - n\varphi/2)], \end{aligned}$$

$$\begin{aligned} T = {} & I_2[\cos(n\pi/2 - n\varphi/2) - \cos(n\pi/2 + n\varphi/2)] \\ & + I_4[\cos(3n\pi/2 - n\varphi/2) - \cos(3n\pi/2 + n\varphi/2)]. \end{aligned}$$

To determine the impedance matrix z, we take the potential differences between the equally-spaced terminals, i.e., $U(\beta,\pi/2) - U(\beta,0)$, $U(\beta,\pi) - U(\beta,\pi/2)$, $U(\beta,3\pi/2) - U(\beta,\pi)$ and $U(\beta,0) - U(\beta,3\pi/2)$, and then sum up the series in Eq. (A2) for a sufficient number of terms.

*Electronic address: mmp24@cam.ac.uk

[1] For a review, see M. B. Isichenko, Rev. Mod. Phys. **64**, 961 (1992).
[2] An extensive list of formulas is contained in: J. A. Reynolds and J. M. Hough, Proc. Phys. Soc., London, Sect. A **70**, 769 (1957).
[3] Y. A. Dreizin and A. M. Dykhne, Sov. Phys. JETP **36**, 127 (1973).
[4] M. B. Isichenko and Ya. L Kalda, Sov. Phys. JETP **55**, 1180 (1982).
[5] B. Y. Balagurov, Sov. Phys. JETP **55**, 1180 (1982).
[6] R. Xu, A. Husmann, T. F. Rosenbaum, M.-L. Saboungi, J. E. Enderby, and P. B. Littlewood, Nature (London) **390**, 57 (1997).
[7] A. Husmann, J. B. Betts, G. S. Boebinger, A. Migliori, T. F. Rosenbaum, and M.-L. Saboungi, Nature (London) **417**, 421 (2002).
[8] M. Lee, T. F. Rosenbaum, M.-L. Saboungi, and H. S. Schnyders, Phys. Rev. Lett. **88**, 066602 (2002).
[9] H. S. Schnyders, M.-L. Saboungi, and T. F. Rosenbaum, Appl. Phys. Lett. **76**, 1710 (2000).
[10] Z. Ogorelec, A. Hamzic, and M. Basletic, Europhys. Lett. **46**, 56 (1999).
[11] B. Q. Liang, X. Chen, Y. J. Wang, and Y. J. Tang, Phys. Rev. B **61**, 3239 (2000).
[12] I. S. Chuprakov and K. H. Dahmen, Appl. Phys. Lett. **72**, 2165 (1998).
[13] M. von Kreutzbruck, B. Mogwitz, F. Gruhl, L. Kienle, C. Korte, and J. Janek, Appl. Phys. Lett. **86**, 072102 (2005).
[14] G. Beck, C. Korte, J. Janek, F. Gruhl, and M. Kreutzbruck, J. Appl. Phys. **96**, 5619 (2004).
[15] S. S. Manoharan, S. J. Prasanna, D. Elefant-Kiwitz, and C. M. Schneider, Phys. Rev. B **63**, 212405 (2001).
[16] C. Kittel, *Quantum Theory of Solids* (Wiley, New York, 1963).
[17] R. A Smith, *Semiconductors*, 2nd ed. (Cambridge University Press, Cambridge, 1978).
[18] A. A. Abrikosov, Phys. Rev. B **58**, 2788 (1998).
[19] A. A. Abrikosov, Europhys. Lett. **49**, 789 (2000).
[20] B. Y. Balagurov, Sov. Phys. Solid State **28**, 1694 (1986).
[21] D. Stroud and F. P. Pan, Phys. Rev. B **13**, 1434 (1976).
[22] D. J. Bergman and D. G Stroud, Phys. Rev. B **62**, 6603 (2000).
[23] C. Herring, J. Appl. Phys. **31**, 1939 (1960).
[24] A. M. Dykhne, Sov. Phys. JETP **32**, 348 (1971).
[25] B. Y. Balagurov, Sov. Phys. Solid State **20**, 1922 (1978).
[26] V. Guttal and D. Stroud, Phys. Rev. B **71**, 201304(R) (2005).
[27] M. M. Parish and P. B. Littlewood, Nature (London) **426**, 162 (2003).
[28] S. A. Solin, T. Thio, D. R. Hines, and J. J. Heremans, Science **289**, 1530 (2000).
[29] T. Zhou, S. A. Solin, and D. R. Hines, Appl. Phys. Lett. **78**, 667 (2001).
[30] A. K. Sarychev, D. J. Bergman, and Y. M. Strelniker, Phys. Rev. B **48**, 3145 (1993).
[31] The effects of boundaries on a sample's resistance are removed by performing a four-probe measurement, where the voltage probes are separate from the electrodes that supply the current, unlike the two-probe resistance measurement considered in this paper.
[32] A. B. Pippard, *Magnetoresistance in Metals* (Cambridge University Press, Cambridge, 1989).
[33] R. S. Popović, *Hall Effect Devices: Magnetic Sensors and Characterization of Semiconductors* (Hilger, Bristol, 1991).
[34] R. F. Wick, J. Appl. Phys. **25**, 741 (1954).
[35] See, e.g., B. P. Paneah, *The Oblique Derivative Problem: The Poincaré Problem* (Wiley-VCH, Berlin, 2000).
[36] R. W. Rendell and S. M. Girvin, Phys. Rev. B **23**, 6610 (1981).
[37] Z.-M. Li and S. P. McAlister, J. Appl. Phys. **66**, 680 (1989).
[38] J. Moussa, L. R. Ram-Mohan, J. Sullivan, T. Zhou, D. R. Hines, and S. A. Solin, Phys. Rev. B **64**, 184410 (2001).
[39] M. B. Isichenko and J. Kalda, J. Mosc. Phys. Soc. **2**, 55 (1992).
[40] G. L. J. A. Rikken, J. A. M. M. van Haaren, W. van der Wel, A. P. van Gelder, H. van Kempen, P. Wyder, J. P. André, K. Ploog, and G. Weimann, Phys. Rev. B **37**, 6181 (1988).
[41] G. J. C. L. Bruls, J. Bass, A. P. van Gelder, H. van Kempen, and P. Wyder, Phys. Rev. Lett. **46**, 553 (1981).
[42] G. J. C. L. Bruls, J. Bass, A. P. van Gelder, H. van Kempen, and P. Wyder, Phys. Rev. B **32**, 1927 (1985).
[43] A. D. Rata, V. Kataev, D. Khomskii, and T. Hibma, Phys. Rev. B **68**, 220403(R) (2003).
[44] Q. Z. Xue, X. Zhang, and D. D. Zhu, Physica B **334**, 216 (2003).
[45] D. P. Young, R. G. Goodrich, J. F. Ditusa, S. Guo, P. W. Adams, J. Y. Chan, and D. Hall, Appl. Phys. Lett. **82**, 3713 (2003).
[46] T. Rötger, G. J. C. L. Bruls, J. C. Maan, P. Wyder, K. Ploog, and G. Weimann, Phys. Rev. Lett. **62**, 90 (1989).
[47] S. H. Simon and B. I. Halperin, Phys. Rev. Lett. **73**, 3278 (1994).
[48] Y. Sun, M. B. Salamon, M. Lee, and T. F. Rosenbaum, Appl. Phys. Lett. **82**, 1440 (2003).
[49] J. P. Heremans, C. M. Thrush, and D. T. Morelli, Phys. Rev. Lett. **86**, 2098 (2001).